SLUJST
Sule Lamido University Journal of Science & Technology Vol. 8 No. 1 [June, 2024], pp. 62-76
https://doi.org/10.56471/slujst.v7i.486
Online ISSN: 2736-0903
Print ISSN: 2736-089X
www.slujst.edu.ng

Structural And Optical Properties of Zinc Borotellurite Glass System Doped with Holmium Trivalent Ion (Ho^{3+})

Mannir Dahiru[1*], Abdullahi Usman[1], and D. G. Diso[1]
[1]Department of Physics Aliko Dangote University of Science & Technology, Wudil
mannirdahiru36@gmail.com[*]

[*]Correspondence Author

Abstract

A glass network system of Holmium doped Zinc borotellurite glass with chemical formula $\{((TeO_2)_{0.7}\ (B_2O_3)_{0.3})_{0.7}\ (ZnO)_{0.3}\}_{1-x}\ (Ho_2O_3)_x$ *where x = 0.005, 0.01, 0.02, 0.03 and 0.04 Molar fraction was prepared by using conventional melt-quenching method. X-ray diffraction analysis (XRD) and Fourier Transform infrared analysis (FTIR) were used to determine the structural properties of the fabricated glass. XRD results confirmed that the prepared glass is amorphous. Density and molar volume of the glass were measured and calculated. The values of the density increase with increase of dopant concentration while molar volume decreases accordingly. The crystalline volume, oxygen molar volume, excess volume and oxygen packing density are also calculated to confirm the structural properties of the fabricated glass. Ultraviolet visible spectroscopy analysis (UV–Vis) was used to determine the optical properties of the prepared glass. The refractive index, molar refraction, molar electronic polarizability, metallization criterion, indirect optical energy band gap, Urbach energy, polaron radius and optical basicity were also calculated and analyzed. The refractive index was found to increase with increase of holmium ion* Ho^{3+} *concentration, optical energy band gap decreases while electronic polarizability increases in conformity with increase of refractive index as the concentration of the dopant increases.*

Keywords: *Holmium oxide, Borotellurite glass, Refractive index, Optical band gab energy and Urbach energy.*

1. Introduction

For quite some years now, research in various capacities are being carried out on the applicability of tellurite glasses in various areas of glass applications such as photonics, optoelectronics, fiber optics and so on (Halimah, Umar, et al., 2019; Usman et al., 2018). A lot of advances have been made and results obtained from such researches show that the tellurite glasses have a lot of advantages over others due to their optical, structural and physical nature.

The previous works, tellurium oxide is combined with either a network former and/or a metallic network modifier to improve the quality and the network formation as tellurium alone does not form glass. Thus, tellurium is regarded as conditional glass network former. It was reported that addition of tellurite to other network formers such as B_2O_3 improves the network structure and hence improves the physical, structural and the optical properties of the glass. If tellurite combined with borates, borotellurite glasses are formed which are now intensively studied for their practical applications, and influenced the quality, transparency and refractive index of the resulted glass system (Usman et al., 2018). Addition of ZnO to borotellurite glass network produces stability and increasing glass forming ability (Kundu et al., 2014). Glasses containing B_2O_3 and ZnO have a long infrared cut off and third order nonlinear optical susceptibility which make them ideal candidate for application as infrared trans- mission components and photonic devices. ZnO is a wide band gap semiconductor that is considered as an important multifunctional material due to its specific chemical surface and micro structural properties.

ZnO can enter into the glass network either in the form of glass former, modifier or both. Nowadays doping inorganic glasses with rare-earth (RE) ions is receiving much attention from researchers. This is because rare-earth ions are extensively used to improve the physical and optical properties of host glasses due to their unique spectroscopic properties resulting from their optical transitions in the intra 4f shell (Usman et al., 2018).

Sule Lamido University Journal of Science & Technology Vol. 8 No. 1 [June, 2024], pp. 62-76
https://doi.org/10.56471/slujst.v7i.486
Online ISSN: 2736-0903
Print ISSN: 2736-089X
www.slujst.edu.ng

The important of the present work is to study the influence of Holmium ion Ho^{+3} on the structural and linear optical properties of Zinc borotellurite glass system. The network structure of the glass system formed was studied using Fourier transform infrared spectroscopy (FTIR) analysis. The influence of Holmium ions on the density, molar volume, Urbach energy and indirect optical energy band gaps were analyzed.

Table 1: Structural and Optical parameters of $\{((TeO_2)_{0.7}\ (B_2O_3)_{0.3})_{0.7}\ (ZnO)_{0.3}\}_{1-x}\ (Ho_2O_3)_x$ Glass system for different values of x

Parameters	x = 0.005	x= 0.01	x = 0.02	x= 0.03	x = 0.04
$\rho(g/cm^3)$ ±0.0168	4.5567	4.6296	4.6965	4.8588	4.9659
$V_m(cm^3/mol)$ ±0.0162	26.0146	25.8864	26.0726	25.7381	25.7078
$V_o(cm^3/mol)$ ±0.0179	13.5814	13.4762	13.4965	13.2486	13.1592
$V_c(cm^3/mol)$ ±0.0298	24.1917	24.2959	24.5043	24.7128	24.9212
$V_{excess}(cm^3/mol)$ ± 0.0433	1.8229	1.5905	1.5683	1.0253	0.7866
OPD(g/atm) ±0.1004	73.6299	74.2050	74.0931	75.4796	75.9925
E_{opt}(eV) ± 0.0298	2.3581	2.7217	2.8990	3.0320	3.0458
ΔE (eV) ± 0.0285	0.3657	0.3557	0.2620	0.2301	0.2192
n ± 0.0076	2.5955	2.4764	2.4248	2.3885	2.3848
R_m ± 0.0529	17.0819	16.3370	16.1463	15.7166	15.6753
Met. Criterion M ± 0.0019	0.3434	0.3689	0.3807	0.3894	0.3903

2. Experimental Method

Holmium doped Zinc borotellurite glass system with chemical composition. $\{((TeO_2)_{0.7}\ (B_2O_3)_{0.3})_{0.7}\ (ZnO)_{0.3}\}_{1-x}\ (Ho_2O_3)_x$ where x = 0.005, 0.01, 0.02, 0.03 and 0.04 M fraction was synthesized by using conventional melt-quenching method. The chemical powder of Tellurium (IV) oxide, TeO2 (99.99%, Alfa Aesar), Boron oxide, B2O3 (98.50%, Alfa Aesar), Zinc oxide, ZnO (99.99%, Alfa Aesar) and Holmium (III) oxide, Ho2O3 (99.50%, Alfa Aesar) were weighted in accordance with calculated compositions using digital weighing machine with an accuracy of ± 0.001g.

The weighted chemicals powder was put in an alumina crucible and stirred with glass rod for 45 minutes in order to obtain homogeneous mixture. The alumina crucible and its content were then transferred to an electric furnace for the pre-heating process at 400 °C for a period of 1 hour to ensure water content or moisture is removed from the mixture. The alumina crucible was then transferred to another electric furnace at 950 °C for 2 hours melting process. At the same time, polished stainless-steel mould was put at the first electric furnace for the free heating process at 400 °C. After the 2 hours melting process, the molten chemical powder was cast into the pre-heated mould and taken back as soon as possible to the first furnace for 1 hour annealing process at 400 °C. The electric furnace was then switched off and the prepared sample was allowed to cool to room temperature. The sample was then polished using silicon carbide paper to 2 mm thickness in order to obtain flat, parallel and shiny surfaces for optical measurements.

For optical measurement the sample was taken to Ultra-violet visible (UV–Vis) spectroscopy for characterization using UV-1650PC UV–Vis spectrometer (Shimadzu) with the wavelength range from 220 to 1700 nm to obtain the optical absorption.

Some portion of the sample was crushed using a plunger and grinded using pestle and mortar. The acquired fine powder was sent to X-ray diffraction (XRD) and Fourier Transform Infra-Red (FTIR) spectroscopies for structural analysis. The density of the samples was measured at room temperature using Archimedes' principle with distilled water as the immersion liquid. The weights of the samples in the air and the distilled water were measured by a digital densimeter with weighing accuracy of± 0.001 g. The volume and specific gravity of the samples were also measured by the densimeter.

SLUJST
Sule Lamido University Journal of Science & Technology Vol. 8 No. 1 [June, 2024], pp. 62-76
https://doi.org/10.56471/slujst.v7i.486
Online ISSN: 2736-0903
Print ISSN: 2736-089X
www.slujst.edu.ng

3. Results and Discussion

3.1 Density and Molar Volume

Density is explained in terms of the relationship between the mass and volume of the various structural groups present in the glass samples. In other words, density is related to how tightly the atoms are bonded together in the glass network (Ami Hazlin et al., 2017). Density is mainly determined by the chemical composition of the glass systems. The density of the glass is one of the important parameters used to analyze the changes in the structure of the glass systems. Density is used to study the structural compactness and strength of the glass system (Halimah, Eevon, et al., 2019)

The density of the sample was measured by using Electronic Densimeter MD-300S that functioned based on Archimedes' principle with distilled water as immersion fluid (Halimah, Eevon, et al., 2019). The change in density and Ho_2O_3 is plotted in Figure 1. From the figure, the density increases as the amount of Ho_2O_3 is increased. This increment is attributed to the molecular weight of Ho_2O_3 which is the largest among all the other oxides in the glass systems (Ami Hazlin et al., 2017). This makes the glass denser as the dopant increases. This increment of the density indicates that the glass system become more compact as the dopant increases. (Usman et al., 2018).

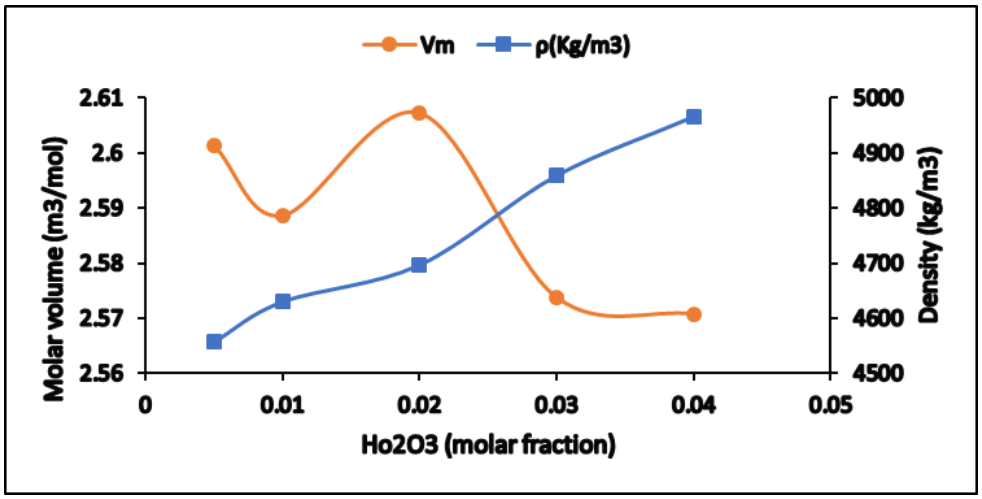

Figure 1: Variation of density and molar volume (V_m) with Ho_2O_3 concentration in $\{((TeO_2)_{0.7}(B_2O_3)_{0.3})_{0.7}(ZnO)_{0.3}\}_{1-x}(Ho_2O_3)_x$ glass system

The molar volume of the glass system decreases as the density increases which shows an opposite behavior to each other (Elkholy et al., 2020). The trends of the density and molar volume with respect to the concentration of the Ho_2O_3 for the prepared glass were shown in Figure 1. From the figure it can observed that the molar volume of the glass sample decreases with the addition of Ho_2O_3. The decrease of the molar volume of the glass system has been expected since the variation of the molar volume is influenced by the rate of change of density and molecular weight. The decrease in molar volume are causes due to the decrease in inter-atomic spacing and bond length between the atoms which was associated with the increment of the stretching force constant of the bonds inside the glass network (Nazrin et al., 2018).

In glass systems, the density of the glass and the molar volume are calculated using the fallowing relations;

$$\rho_s = \frac{m_a}{V} \quad (1)$$

$$V_m = \sum \frac{X_i M_i}{\rho} \quad (2)$$

Sule Lamido University Journal of Science & Technology Vol. 8 No. 1 [June, 2024], pp. 62-76
https://doi.org/10.56471/slujst.v7i.486
Online ISSN: 2736-0903
Print ISSN: 2736-089X
www.slujst.edu.ng

Where ρ_s, M_g, X_i, M_i and V_m are density of the glass, molecular weight of the glass systems, molar fraction, molecular weight of *i*th component and molar volume of the glass systems respectively. The values of V_m and ρ are presented in Table 1 while their inverse behaviors are illustrated in Fig. 1.

Oxygen molar volume and crystalline volume were also calculated and presented in Table 1. Oxygen molar volume (V_o), Crystalline volume (V_c) and Excess volume (V_{excess}) were calculated using the following Equations and are illustrated in Figures 2 and 3.

$$V_o = \frac{V_m}{\sum_i X_i n_i} \quad (3)$$

$$V_c = \sum_i X_i V_i \quad (4)$$

$$V_{excess} = V_m - V_c \quad (5)$$

V_i is the molar volume of *i*th component in crystalline phase (i.e. V_i = 28.1479, 28.3001, 14.5061 and 44.9297 cm^3/mol for α-TeO_2, B_2O_3, ZnO and Ho_2O_3 respectively using their corresponding crystalline densities of 5.67, 2.46, 5.61 and 8.41 g/cm^3)

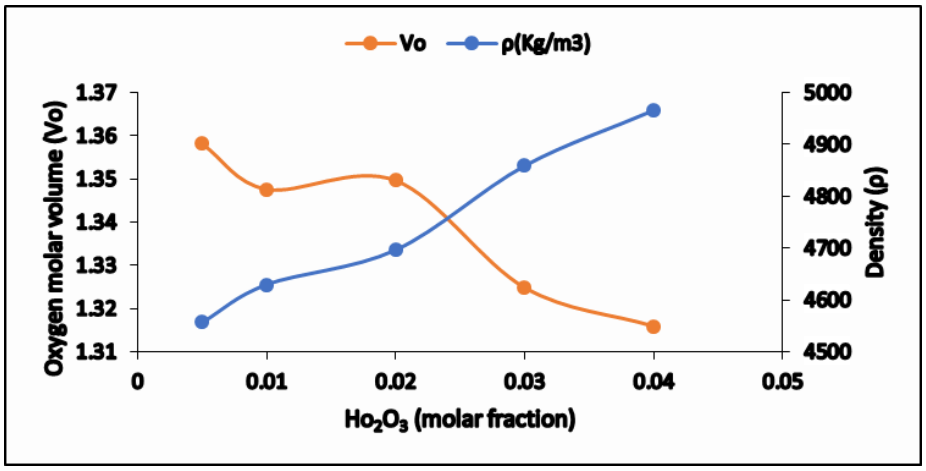

Figure 2: Variation of oxygen molar volume (V_o), density (ρ) with Ho_2O_3 concentration $\{((TeO_2)_{0.7}(B_2O_3)_{0.3})_{0.7}(ZnO)_{0.3}\}_{1-x}(Ho_2O_3)_x$ glass system

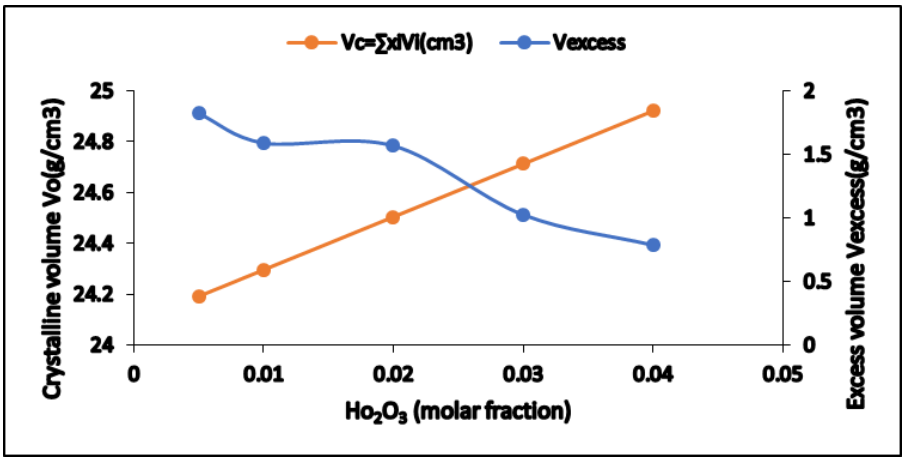

Figure 3: Variation of crystalline volume (V_c) and excess volume (V_{excess}) with Ho_2O_3 concentration $\{((TeO_2)_{0.7}(B_2O_3)_{0.3})_{0.7}(ZnO)_{0.3}\}_{1-x}(Ho_2O_3)_x$ glass system.

Sule Lamido University Journal of Science & Technology Vol. 8 No. 1 [June, 2024], pp. 62-76
https://doi.org/10.56471/slujst.v7i.486
Online ISSN: 2736-0903
Print ISSN: 2736-089X
www.slujst.edu.ng

The measurement of the tightness of packing of the oxides network known as Oxygen Packing Density (OPD) was calculated using the relation below, Figure 4 illustrates the variation of oxygen packing density with Ho_2O_3 concentration.

$$OPD = n \times \frac{\rho}{M} \times 1000 \quad (6)$$

Where n is the number of oxygen in the composition, ρ the density of desired glass samples and M is the molecular weight of the sample.

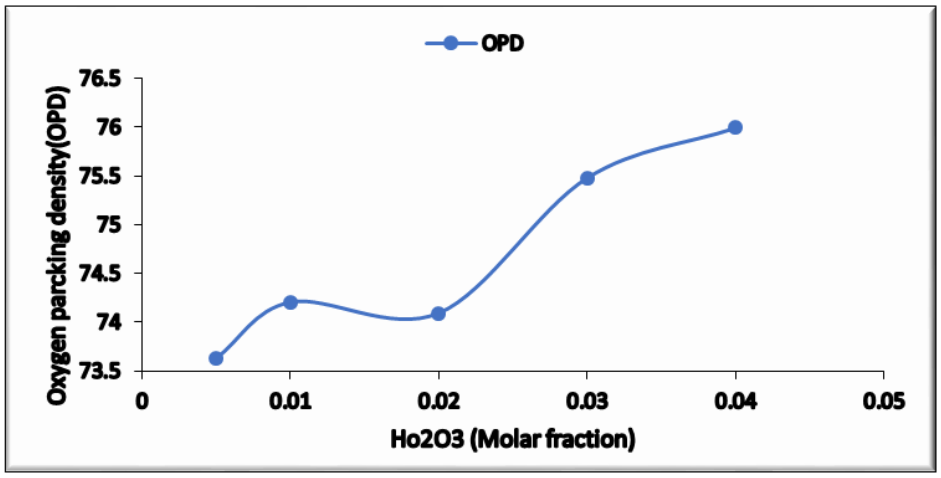

Figure 4: The variation of oxygen packing density (OPD) with Ho_2O_3 concentration of $\{((TeO_2)_{0.7}\ (B_2O_3)_{0.3})_{0.7}\ (ZnO)_{0.3}\}_{1-x}\ (Ho_2O_3)_x$ glass system.

3.2 X- Ray Diffraction (XRD) and Fourier Transform Infra-Red Analysis (FTIR)

The XRD spectra of zinc borotellurite glass systems doped with Ho_2O_3 is illustrated in Figure 5. The X-ray diffraction patterns for the zinc borotellurite glass systems doped with Ho_2O_3 are measured for the five different molar fraction content. The XRD result shows a broad diffuse diffraction curve around $2\theta = 30°$ which confirms the amorphous nature of the glass sample. It also shows lack of long range atomic order lines in the glass network (Hamza, Halimah, Muhammad, Chan, et al., 2019; S. A. Umar et al., 2017a).

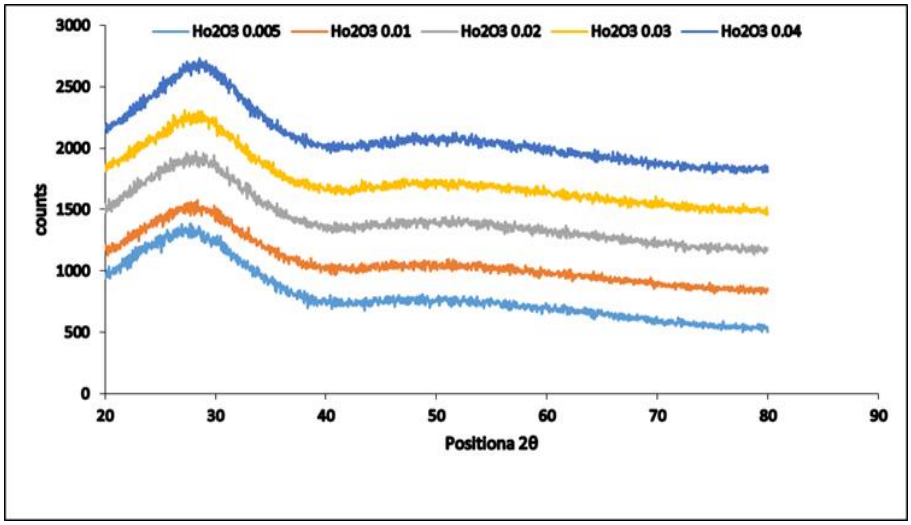

Figure 5: XRD diffraction pattern of $\{((TeO_2)_{0.7}\ (B_2O_3)_{0.3})_{0.7}\ (ZnO)_{0.3}\}_{1-x}\ (Ho_2O_3)_x$ glass system with different concentration of Holmium ions

SLUJST
Sule Lamido University Journal of Science & Technology Vol. 8 No. 1 [June, 2024], pp. 62-76
https://doi.org/10.56471/slujst.v7i.486
Online ISSN: 2736-0903
Print ISSN: 2736-089X
www.slujst.edu.ng

Fourier transform infrared (FTIR) is used to confirm the presence or absence of functional groups in the glass network systems (Ami Hazlin et al., 2017). The ability of identifying molecules in a material is related to the vibrational mode of molecules whereby each and every molecule possesses different vibrational mode which differentiates a molecule from other molecules. The vibration of a molecular group in a glass matrix is independent on the vibration of other molecular group since the wavenumber where each of the molecular group vibrate is distinct (Faznny et al., 2020).

The FTIR spectra of Zinc borotellurite glass doped with Holmium oxide were shown in Figure 6. The five observable vibration bands which are on the range of 623 – 640, 689 – 703, 880 – 920, 1210 – 1223 and 1340 – 1382 cm^{-1}. The detected functional vibrational groups and their respective assignment are recorded in Table 3. The TeO_3 and BO_3 are detected in the FTIR spectra, this means that the Ho_2O_3 element only break the bond of boron oxide and tellurium oxide.

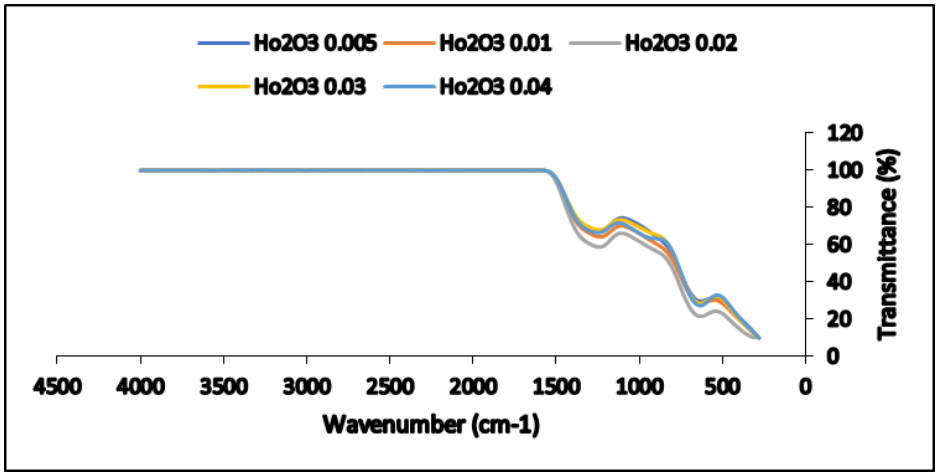

Fig. 6. FTIR Spectra of $\{((TeO_2)_{0.7}(B_2O_3)_{0.7}(ZnO)_{0.3}\}_{1-x}(Ho_2O_3)_x$

The divided frequencies in infrared spectra regions confirm the vibrational linkage between the oxides. The lower energy region 640cm^{-1} consists of the vibration of B – O – B linkage. The intermediate energy region in the region of 1210 – 1223cm^{-1} of the infrared region stand for B – O bond stretching BO_4 in BO_4 groups, the higher region 1320 – 1450cm^{-1} belong to the vibration of the B – O bond in the BO_3 groups.

The two structure of the tellurium that contribute to the tellurite glass network are trigonal pyramid (TeO_3) and trigonal bipyramid (TeO_4). The broad peaks appeared in the FTIR are referred to the mixing structure of TeO_3 groups, symmetry TeO_4 groups and deformed TeO_4 groups. The absorption of TeO_3 groups has a higher frequency position than the TeO_4 groups (Ami Hazlin et al., 2017). The first group of bond that exists around 623 – 640cm^{-1} is related to TeO_4 trigonal bipyramid and the second group of bond formed around 689 – 703cm^{-1} crosspond to the TeO_3 trigonal pyramid (Halimah et al., 2017)

The functional vibration groups (in cm^{-1}) of the Ho_2O_3 doped Zinc borotellurite glass at different molar fraction is shown in the Table 2.

Table 2: Functional vibration groups (in cm^{-1}) of the Ho_2O_3 doped zinc borotellurite glasses at different molar fraction

S/N	Band frequency range (cm^{-1})	Assignment
1	623 – 640	Te–O bond stretching in the TeO_4 Units (trigonal bipyramid) (Faznny et al., 2020)
2	689 – 703	Formation of Te – O bond in TeO_3 Units (trigonal pyramid) (Halimah et al., 2017)

SLUJST
Sule Lamido University Journal of Science & Technology Vol. 8 No. 1 [June, 2024], pp. 62-76
https://doi.org/10.56471/slujst.v7i.486
Online ISSN: 2736-0903
Print ISSN: 2736-089X
www.slujst.edu.ng

3	880 – 920	B – O B Linkage (Azlina et al., 2019)
4	1210 – 1223	B – O bond stretching in BO_4 groups. (Halimah, Eevon, et al., 2019)
5	1340 – 1382	B – O bond in BO_3 groups. (S. A. Umar et al., 2017a)

3.3 Polaron Radius (R_p)

Polaron is a quasi-particle formed by a conduction electron or hole in a polar semiconductors, ionic crystals or alkali oxides/halides with its self-induced polarization. Polarons are studied to describe the polar interaction between an electron and the longitudinal optical phonons. The polaron radius is the linear atomic/ionic displacement field of a polaron (S. A. Umar et al., 2017b). When the polaron radius is of the order of the lattice constant, the polaron is called small polaron. When the radius is much larger than the lattice constant of the material, the polaron is termed as large polaron. Normally, the decrease in the polaron radius causes increase in the polarizability of a material. As shown in the table3, the value of the polaron radius decreased with increasing concentration of Ho_2O_3 ions in the glass from 8.2691 – 4.1182 Å. The values suggest that the polaron is a small polaron as the values does not exceed the lattice constants of the individual oxides in the glass. The decrease in the polaron radius may be associated to the decreases in the glass polarizability and compactness. This may eventually decrease the glass electrical conductivity

3.4. Internuclear distance (R_i)

The internuclear distance is of significant importance because of its direct relationship to the structure of tellurite doped glasses (Elkholy et al., 2020). In Table 3 it is observed that the values of internuclear distance decreases as the values of Holmium ions concentration is increased. The molar volume increased in the glass network which is connected to the substitution of higher polarized ions (A. Umar et al., 2018).

3.5. Field strength (F)

Field strength is of significant importance because of its direct relationship to structural compactness of the glass system (Kaur et al., 2019). In Table 3, it is observed that the field strength of the prepared glass is increasing. This increase in field strength indicates the increase in polymerization in the glass systems which indicate the strangeness of the glass structure and shows the strong field site of the glass. The prepared glass is believed to be strong based on its field strength (Halimah & Eevon, 2019; Hamza, Halimah, Muhammad, & Chan, 2019; Tanko et al., 2016).

The variation of field strength and refractive loss with the holmium ion concentration was shown in Figure 7 below.

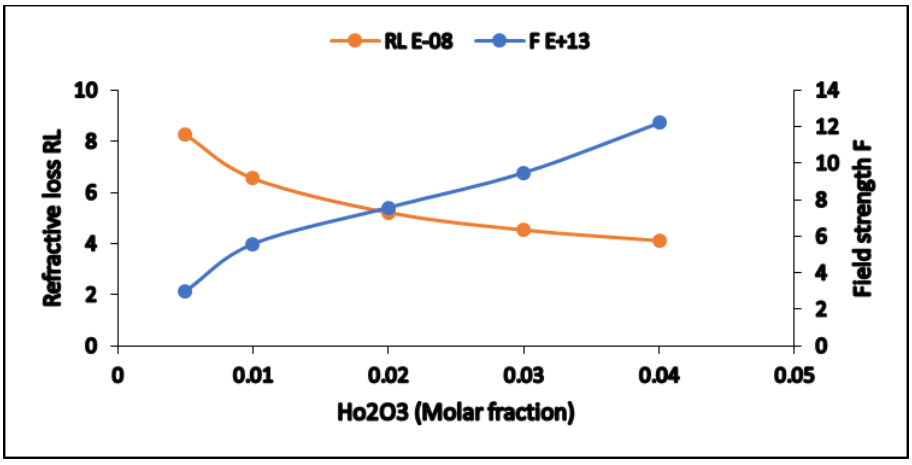

Figure 7: The variation of field strength and refractive loss with Ho_2O_3 concentration of $\{((TeO_2)_{0.7}\ (B_2O_3)_{0.3})_{0.7}\ (ZnO)_{0.3}\}_{1-x}\ (Ho_2O_3)_x$ glass system.

Sule Lamido University Journal of Science & Technology Vol. 8 No. 1 [June, 2024], pp. 62-76
https://doi.org/10.56471/slujst.v7i.486
Online ISSN: 2736-0903
Print ISSN: 2736-089X
www.slujst.edu.ng

3.6. Boron – Boron separation (d_{B-B})

The boron – boron separation helps in explaining the glass compactness and rigidity, from Table4, it is observed that the values of the boron – boron separation decreases from 0.3011 – 0.2990 as the concentration of the Ho_2O_3 increases, this makes the network of the prepared glass more compact and stronger.

Polaron radius (R_p), Internuclear distance (R_i), Field strength (F), Boron–Boron separation (d_{B-B}), Average coordination number (m), Number of bonds per unit volume (n_b) and boron molar volume (V_m^B) can be calculated using the relations bellow:

$$R_p(\text{Å}) = \frac{1}{2}\left(\frac{\pi}{6N}\right)^{\frac{1}{3}} \quad (7)$$

$$F(cm^{-2}) = \left(\frac{Z}{r_p^2}\right) \quad (8)$$

$$R_i(\text{Å}) = \left(\frac{1}{N}\right)^{\frac{1}{3}} \quad (9)$$

$$d_{B-B} = \left(\frac{V_m^B}{N_A}\right)^{\frac{1}{3}} \quad (10)$$

$$m = \sum_i n_{ci} X_i \quad (11)$$

$$n_b = \frac{N_A}{V_m} m \quad (12)$$

$$V_m^B = \frac{V_m}{2(1-X_B)} \quad (13)$$

Where;

Z = atomic number
n_{ci} = Coordination number of cation
X_i = Molar concentration of Ho_2O_3
Where X_B = Molar fraction of boron

Table 3: Field strength (F), polaron radius (R_p), internuclear distance (R_I), average coordination number (m) and number of bonds per unit volume (n_b)

Molar Fraction	F (cm^{-3}) ± 0.3535	R_p (Å) ± 0.01689	Ri(Å) ± 0.0419	m(am.CN) ± 0.0023	n_b ± 0.0111
x = 0.005	2.99802	8.26913	2.0519	4.3981	10.1809
x = 0.01	5.58995	6.55242	1.62592	4.4061	10.2499
x = 0.02	7.58012	5.2131	1.29358	4.4222	10.2139
x = 0.03	9.48367	4.5345	1.12519	44383	10.3844
x = 0.04	12.2052	4.11825	1.0219	4.4544	10.4343

Table 4: Boron- boron separation (d_{B-B}), Transmission coefficient (T), Reflective loss (R_L) and boron molar volume (V^B_M)

X	d_{B-B} ± 0.0001	T ± 0.0021	R_L ± 0.0015	V^B_M ± 0.0239
0.005	0.3011	0.6710	0.1969	2.0519
0.01	0.3005	0.6944	0.1804	2.5886
0.02	0.3010	0.7049	0.1731	2.6073

Sule Lamido University Journal of Science & Technology Vol. 8 No. 1 [June, 2024], pp. 62-76
https://doi.org/10.56471/slujst.v7i.486
Online ISSN: 2736-0903
Print ISSN: 2736-089X
www.slujst.edu.ng

0.03	0.2994	0.7125	0.1679	2.5738
0.04	0.2990	0.7132	0.1674	2.5708

3.7. Refractive index

Refractive index value of a glass is influenced by the interaction of light with the electrons of the constituent atoms of the glass. The refractive index value of fabricated glass samples is calculated using the equation below

$$\frac{n^2-1}{n^2+2} = 1 - \sqrt{\frac{E_{opt}}{20}} \quad (14)$$

Where n is the refractive index and E_{opt} is the value of indirect band gap.

The values of the refractive index that are tabulated in shows a decreasing trend. The decrement in refractive index might be due to the incorporation of modifier that attributed to the decrease in the number of nonbridging oxygen. Thus, the decreasing value of refractive index as amount of holmium oxide increases is due to the decreasing number of high polarizabilities nonbridging oxygen. Refractive index of the fabricated glasses is higher when compared to previous research that obtained the refractive index values in the range of 2.5655 – 2.3848. The variation of refractive index (n) with Ho_2O_3 concentration was shown in Figure 7

3.8. Molar Refraction

Molar refraction is a measure of the total polarizability of a mole of a material. Through Lorentz-Lorenz equation, the relationship between molar refraction, R_m to refractive index and molar volume, V_m for isotropic substance such as liquid, glasses and cubic crystals can be identified (Polosan et al., 2021). The molar reflection was calculated using the relations below

$$R_m = \left[\frac{n^2-1}{n^2+2}\right] V_m \quad (15)$$

Where R_m is the molar refraction, V_m is the molar volume and n is the refractive index.

3.9. Energy Band Gab

The optical band gap, E_{opt} of zinc borotellurite doped with Holmium oxide glass systems were obtained from ultraviolet absorption edges. The studies of the optical band gap near the fundamental absorption edge are the typical methods to gain knowledge on the structural disorders between the host and the impurities when high energy ultraviolet light is absorbed by the glassy phase. The fundamental absorption is referring to the band-to-band transitions and it signifies itself by rapidly rising in the absorption used to determine the optical band gap.

The value of the optical band gap E_{opt} of the glass system are determined by extrapolating the linear region of the curves of $(\alpha\hbar\omega)^{1/2}$ and $(\alpha\hbar\omega)^2$ against $(\hbar\omega)$ (Ami Hazlin et al., 2018), the calculated value of optical band gap for the series of the glass systems are recorded in Table 1. The trend of the optical band gap of zinc borotellurite glass doped with Ho_2O_3 was shown in Figure 10.

It is noticed from Figure 10 that as the concentration of Ho_2O_3 in the glass matrices increases, the optical band gap increases from 2.3581 - 3.0458 eV (Gangwar et al., 2019). It was seen that band gap of tellurite glasses is increasing with increase in modifier content, that is the UV transmittance curve is getting shifted to lower wavelength values. The shift of band gap energies to lower values corresponds to decreasing concentration of NBOs which is confirmed by XRD, in which the electron bound high tightly than the bridging oxygen. The trend of the curve shows that the band edge values of glass samples are shifted to lower energy values due to decrease of NBOs and E_{opt} increased. The nature of curve observed may possibly be due to the conversion of TeO_4 subunits of Tellurium oxide into TeO_3 subunits. As literature states the band energy edges for TeO_3 are greater than TeO_4 with smaller value of wavelengths for TeO_3 than TeO_4. Thus, this blue shift is observed. The decrease in non-bridging

SLUJST
Sule Lamido University Journal of Science & Technology Vol. 8 No. 1 [June, 2024], pp. 62-76
https://doi.org/10.56471/slujst.v7i.486
Online ISSN: 2736-0903
Print ISSN: 2736-089X
www.slujst.edu.ng

oxygen leads to the decrease in degree of disorder in the glass structure. This is seen by the increase in the values of the Urbach energy of the glass samples with increasing concentration of the modifier.

It is stated in Reference (Halimah, Eevon, et al., 2019) that, the decreasing number of non-bridging oxygen is one of the reasons that contribute to an increment in energy band gap values. The number of non-bridging oxygen decreases because of the increasing number of oxygen anions such as TeO_4 that are tightly bound to the host materials. It was shown that the Urbach energy decreases with increase of Ho_2O_3 content. The low Urbach energy is related to the decrease of degree of disorderness in glass structure. In this case, as the concentration of the holmium ion increases, fragility and Urbach energy decreases due to the decreasing number of nonbridging oxygen and BO_3 units in the glass system.

According to Nazrin et al., (2018) the value of band gap increases as the value of the concentration of the rare earth is increased. In this study it was observed that value of the band gap increases from 2.3581 - 3.0458 eV. This behavior may be associated to the structural changes that occur after the addition of Ho_2O_3 as reported (Asyikin et al., 2020). The increases in direct and indirect energy band gap are caused by the formation of NBO in the glass network which causes the glass structure to become less order. The addition of Ho_2O_3 causes the breaking of regular structure of tellurite which leads to the increase in energy band gap.

According to Elazoumi et al., (2018), Asyikin et al., (2020) and Usman et al., (2018) the absorption coefficient, α(ω) and photon energy, ħω of the incident radiation are related to each other by the following equation:

$$\alpha(w) = \frac{B(\hbar\omega - E_{opt})^n}{\hbar\omega} \tag{16}$$

Where n is an index that takes different values, 1/2, 2, 3/2, and 3 depending on the mechanism of inter band transitions. These values correspond to direct allowed, indirect allowed, direct forbidden and indirect forbidden transitions respectively. B is a constant ($B \neq 0$ for amorphous materials) known as band tailing parameter and E_{opt} is the optical band gap energy. The value of absorption coefficient, α(ω) is generated from the absorbance of the glass sample at different wavelengths of incident radiation, using the following relation:

$$\alpha(w) = 2.303\frac{A}{t} \tag{17}$$

Where t is the thickness of the sample and A represents the absorbance. By rearranging Eq. (16) the following equations are obtained:

$$\alpha\hbar\omega = B(\hbar\omega - E_{opt})^n \tag{18}$$

$$(\alpha\hbar\omega)^{\frac{1}{n}} = B(\hbar\omega - E_{opt}) \tag{19}$$

A plot of $(\alpha\hbar\omega)^{1/n}$ against ħω is called Tauc's plot and is used to estimate the optical band gap energy of a given transition.

If $(\alpha\hbar\omega)^{1/n} = 0$, i.e. along ħω axis, Eq. 22 becomes $B(\hbar\omega - E_{opt}) = 0$. Since from the previous condition $B \neq 0$, it can be concluded that $(\hbar\omega - E_{opt}) = 0$. Hence $E_{opt} = \hbar\omega$, which means that optical band gap energy takes the value of photon energy. This is practically obtained by extrapolating the linear portion of the curve of the corresponding Tauc's plot to meet ħω axis. The value of E_{opt} obtained depends on the mechanism of the glass transition, which is determined by the value of n. The spectral dependence of the absorption coefficient α(ω) on photon energy ħω is expressed by Urbach empirical rule, which is given by the following equation:

$$\alpha(\omega) = Bexp^{\frac{\hbar\omega}{\Delta E}} \tag{20}$$

Sule Lamido University Journal of Science & Technology Vol. 8 No. 1 [June, 2024], pp. 62-76
https://doi.org/10.56471/slujst.v7i.486
Online ISSN: 2736-0903
Print ISSN: 2736-089X
www.slujst.edu.ng

ΔE denotes the energy of the band tail known as Urbach energy. This energy is weakly dependent upon temperature and is often interpreted as the width of the band tail due to localized states in the band gap of disordered or low crystalline materials (Eevon et al., 2016). In the glass materials, the Urbach energy, ΔE exists in the forbidden energy band gap. The Urbach energy parameter is used to determine the disorder of the material and can be estimated by using Urbach equation (Halimah et al., 2018; Halimah, Eevon, et al., 2019; S. A. Umar et al., 2017a).

The variation of the Urbach energy with respect to the molar fraction is shown in Figure 7. It can be seen from the figure that the Urbach energy values decrease with the increase in Ho_2O_3 concentration from 0.3657 to 0.2192 eV. From the result, it can be inferred that the Urbach energy values are inversely proportional to the optical band gaps. In this study, the glass with higher Ho_2O_3 content has lower Urbach energy. The materials with lower Urbach energy indicate that the materials have lower tendency to convert the weak bonds into defect.

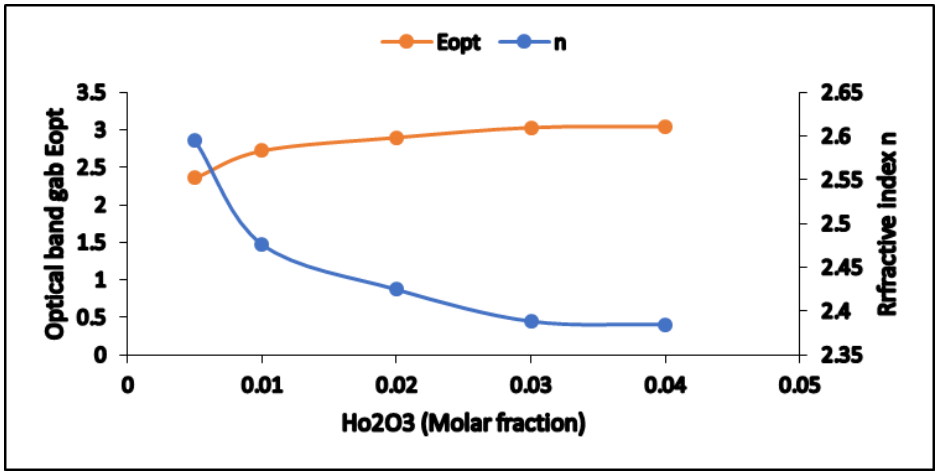

Fig. 8. Variation of optical band gab (E_{opt}), refractive index (n) with Ho_2O_3 Concentration of $\{((TeO_2)_{0.7}(B_2O_3)_{0.3})_{0.7}(ZnO)_{0.3}\}_{1-x}(Ho_2O_3)_x$ glass system with different concentration of Holmium ions

3.10. Metallization Criterion

Metallization criterion is theoretically calculated to determine the tendency for metallization and to investigate the insulating behavior of the fabricated glasses. M.K. Halima has proposed the theory on metallization of the condensed matter that explained that the refractive index become infinite for the condition $R_m/V_m = 1$ in the Lorentz-Lorenz equation. Materials with the condition $R_m/V_m = 1$ or Rm/Vm> 1 have mobile electron and the system of the materials are predicted to be metallic in nature while materials with the condition $R_m/V_m < 1$ are predicted to have non-metallic nature. Subtracting by 1 gives the metallization criterion, M: Metallization criterion on the basis of refractive index, and energy band gap, M(E_g) have been calculated (Dimitrov & Sakka, 1996) by using Equation 25 and are shown in Table 1 and are plotted as a function of Ho_2O_3 concentration. Both the refractive index based and energy band gap-based metallization criteria increase with increasing Ho_2O_3 concentration. This indicates that the tendency for metallization in the electronic structure is low in the fabricated glasses. The increasing trend in metallization criterion on the basis of band gap energy indicates that the samples are not metalizing and the width of conduction bands becomes smaller. The variation of the metallization criterion with the holmium ion concentration is shown in figure 9 below

Sule Lamido University Journal of Science & Technology Vol. 8 No. 1 [June, 2024], pp. 62-76
https://doi.org/10.56471/slujst.v7i.486
Online ISSN: 2736-0903
Print ISSN: 2736-089X
www.slujst.edu.ng

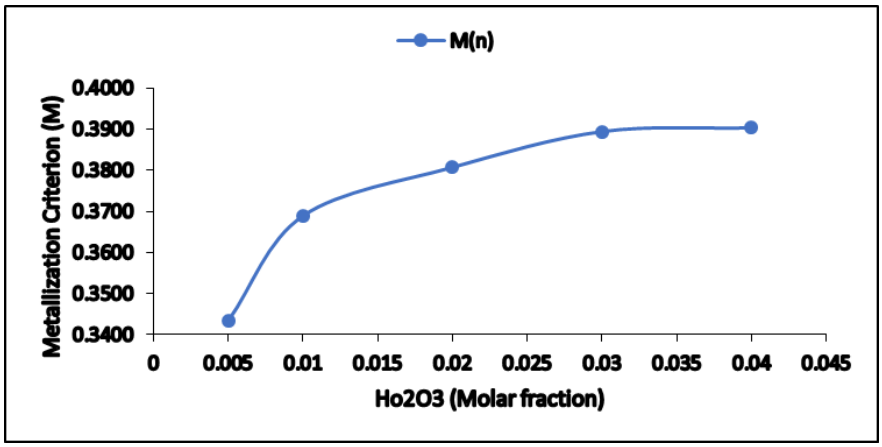

Figure9. Variation of metallization criterion with Ho_2O_3 Concentration of $\{((TeO_2)_{0.7}(B_2O_3)_{0.3})_{0.7}(ZnO)_{0.3}\}_{1-x}(Ho_2O_3)_x$ glass system with different concentration of Holmium ions

$$M = 1 - \frac{R_m}{V_m} \qquad (21)$$

Metallization criterion of any material tells about the non-metallic nature of the material on the basis of its band gap energy and is obtained as reported by (S. A. Umar et al., 2017a)

As shown in Table 2 , the metallization criterion (M) for the studied glasses are in the range of 0.3434–0.3903 (Ami Hazlin et al., 2018). The obtained values correspond to metallization criterion of oxide glasses with good optical non-linearity. Thus, the glass will be good for non-linear optical application (Azlina et al., 2019). Metallization criterion have been calculated (Dimitrov & Sakka, 1996) by using equation 21 above.

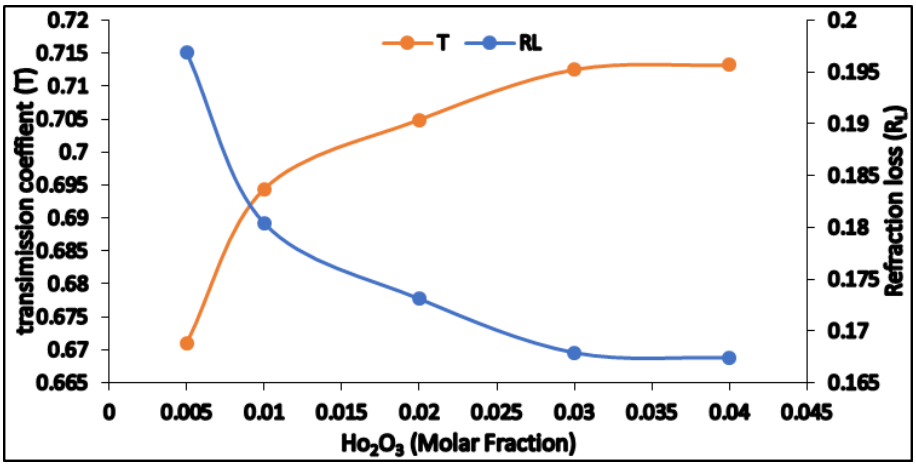

Figure 10. Variation of Transmission Coefficient (T) and Refractive loss (R_L) with Ho_2O_3 Concentration of $\{((TeO_2)_{0.7}(B_2O_3)_{0.3})_{0.7}(ZnO)_{0.3}\}_{1-x}(Ho_2O_3)_x$ glass system with different concentration of Holmium ions

4. Conclusion

In the present study on zinc borotellurite glasses system, the effects of holmium oxide ion on structural and optical properties were measured and analyzed. The Ho^{3+} ions doped zinc borotellurite glasses with the following chemical formula $\{((TeO_2)_{0.7}(B_2O_3)_{0.3})_{0.7}(ZnO)_{0.3}\}_{1-x}(Ho_2O_3)_x$ were prepared at various doping concentration of Ho_2O_3 and characterized by using, X-ray diffraction (XRD) and Fourier transform infrared (FTIR) techniques in order to explore their physical and structural properties. The amorphous nature of the glass samples is confirmed

Online ISSN: 2736-0903
Print ISSN: 2736-089X
www.slujst.edu.ng

by the observed XRD patterns. The nonexistence of the sharp peaks from the XRD spectra obtained from the XRD measurement confirms the amorphous nature of the glass systems which shows the lack of long-range atomic order lines in the glass network. The FTIR results show five distinct transmission bands which belongs to the TeO_4, TeO_3, BO_4 and BO_3 vibrational units, this means that this means that the Ho_2O_3 element only break the bond of boron oxide and tellurium oxide.

The density and molar volume show opposite trends with the increase of Ho_2O_3 concentration. The density increases while molar volume decreases accordingly. The decrease in oxygen molar volume, molar volume together with the increase in oxygen packing density (OPD) as the concentration of the dopant increases confirm the decrease in the formation of NBO. Hence the excess volume of the glass network decreases which favors the formation of tightly packed glass structure. The FTIR of the prepared glass system indicates that TeO_2 exists as TeO_3 and TeO_4 structural units. But the number of TeO_3 decreases with the increase of Ho_2O_3 content and TeO_4 is observed in all the samples which confirmed the transformation of TeO_3 structural units into TeO_4 structural units. Holmium plays the role of network modifier and B_2O_3 exists in the form of BO_3 trigonal and BO_4 tetrahedral structural units. The shift of the absorption edge, the increase of the optical band gap energy (E_{opt}) and the decrease of refractive index are attributed to the decrease in the concentration of NBO atoms. The values of Urbach energy increase with the increase in the concentration of Ho_2O_3 which indicates that the glass system has more defects. The metallization criterion of the glass system was found within the range of 0.3434 – 0.3903, hence they can serve as non-linear optical materials. Polarons are studied to describe the polar interaction between an electron and the longitudinal optical phonons. The decrease in the polaron radius may be associated with the increase in the glass polarizability and compactness. This may eventually increase the glass electrical conductivity.

5. Recommendations for Future Research

The recent research on zinc borotellurite glass systems doped with Ho_2O_3 can be further investigated. The work reported in this current research is based on the understanding in a few measurements in the physical, structural, optical and polarizability properties of the glass systems. However, more aspects need to be further investigated in order to enhance the properties of the glass systems. Some of the aspects are:

A. Magnetic properties

Holmium ion is a magnetically active ion and Ho_2^{+3} ion which has unpaired electron might result in the additional magnetic interactions and modification on the structure of the glass materials. The study of the magnetic properties of the glass materials is a must in order to widen the application of the glass materials.

B. Elastic properties

Elastic properties of the glass systems are important in order to determine the strength of the material when force is applied to the glass materials some elastic parameters that might need to be considered are elastic moduli, Poisson's ratio and microhardness.

C. Thermal properties

Thermal properties can be investigated in order to observe the ability of the glass samples to conduct heat. The study on the thermal properties in solid state lighting is important to understand the major thermal resistance for heat dissipation. Some parameters that are included in the thermal properties are heat capacity, thermal expansion, thermal conductivity and thermal strength.

References

Ami Hazlin, M. N., Halimah, M. K., & Muhammad, F. D. (2018). Absorption and emission analysis of zinc borotellurite glass doped with dysprosium oxide nanoparticles for generation of white light. *Journal of Luminescence*, *196*(July 2017), 498–503. https://doi.org/10.1016/j.jlumin.2017.11.054

Ami Hazlin, M. N., Halimah, M. K., Muhammad, F. D., & Faznny, M. F. (2017). Optical properties of zinc borotellurite glass doped with trivalent dysprosium ion. *Physica B: Condensed Matter*, *510*, 38–42.

Online ISSN: 2736-0903
Print ISSN: 2736-089X
www.slujst.edu.ng

https://doi.org/10.1016/j.physb.2017.01.012

Asyikin, A. S., Halimah, M. K., Latif, A. A., Faznny, M. F., & Nazrin, S. N. (2020). Physical, structural and optical properties of bio-silica borotellurite glass system doped with samarium oxide nanoparticles. *Journal of Non-Crystalline Solids*, *529*. https://doi.org/10.1016/j.jnoncrysol.2019.119777

Azlina, Y., Azlan, M. N., Halimah, M. K., Umar, S. A., & Najmi, G. (2019). Optical performance of neodymium nanoparticles doped tellurite glasses. *Physica B: Physics of Condensed Matter*, 411784. https://doi.org/10.1016/j.physb.2019.411784

Dimitrov, V., & Sakka, S. (1996). Electronic oxide polarizability and optical basicity of simple oxides. I. *Journal of Applied Physics*, *79*(3), 1736–1740. https://doi.org/10.1063/1.360962

Eevon, C., Halimah, M. K., Zakaria, A., Azurahanim, C. A. C., Azlan, M. N., & Faznny, M. F. (2016). Linear and nonlinear optical properties of Gd3+ doped zinc borotellurite glasses for all-optical switching applications. *Results in Physics*, *6*(October), 761–766. https://doi.org/10.1016/j.rinp.2016.10.010

Elazoumi, S. H., Sidek, H. A. A., Rammah, Y. S., El-Mallawany, R., Halimah, M. K., Matori, K. A., & Zaid, M. H. M. (2018). Effect of PbO on optical properties of tellurite glass. *Results in Physics*, *8*, 16–25. https://doi.org/10.1016/j.rinp.2017.11.010

Elkholy, H., Othman, H., Hager, I., Ibrahim, M., & Ligny, D. De. (2020). Thermal and optical properties of binary magnesium tellurite glasses and their link to the glass structure. *Journal of Alloys and Compounds*, *823*, 153781. https://doi.org/10.1016/j.jallcom.2020.153781

Faznny, M. F., Halimah, M. K., Eevon, C., Latif, A. A., Muhammad, F. D., Asyikin, A. S., Nazrin, S. N., & Zaitizila, I. (2020). Comprehensive study on the nonlinear optical properties of lanthanum nanoparticles and lanthanum oxide doped zinc borotellurite glasses. *Optics and Laser Technology*, *127*(October 2019), 106161. https://doi.org/10.1016/j.optlastec.2020.106161

Gangwar, H., Singh, V., Tewari, B. S., Gupta, H., & Purohit, L. P. (2019). Study of zinc doped tellurite glasses using XRD, UV-Vis and FTIR. *Materials Today: Proceedings*, *17*, 329–337. https://doi.org/10.1016/j.matpr.2019.06.437

Halimah, M. K., Ami Hazlin, M. N., & Muhammad, F. D. (2018). Experimental and theoretical approach on the optical properties of zinc borotellurite glass doped with dysprosium oxide. *Spectrochimica Acta - Part A: Molecular and Biomolecular Spectroscopy*, *195*, 128–135. https://doi.org/10.1016/j.saa.2017.12.054

Halimah, M. K., & Eevon, C. (2019). Comprehensive study on the effect of Gd 2 O 3 NPs on elastic properties of zinc borotellurite glass system using non-destructive ultrasonic technique. *Journal of Non-Crystalline Solids*, *511*(March 2018), 10–18. https://doi.org/10.1016/j.jnoncrysol.2019.01.033

Halimah, M. K., Eevon, C., Kaur, S., Pandey, O. P., Jayasankar, C. K., Chopra, N., Vijayakumar, M., Jayanthi, P., Marimuthu, K., Halimah, M. K., Asyikin, A. S., Nazrin, S. N., Faznny, M. F., Azlan, M. N., Halimah, M. K., Suriani, A. B., Azlina, Y., El-Mallawany, R., Faznny, M. F., … Nitescu, A. (2019). Spectroscopic, thermal and structural investigations of Dy3+ activated zinc borotellurite glasses and nano-glass-ceramics for white light generation. *Results in Physics*, *143*(May), 156176. https://doi.org/10.1016/j.physb.2017.01.012

Halimah, M. K., Faznny, M. F., Azlan, M. N., & Sidek, H. A. A. (2017). Optical basicity and electronic polarizability of zinc borotellurite glass doped La3+ ions. *Results in Physics*, *7*(January), 581–589. https://doi.org/10.1016/j.rinp.2017.01.014

Halimah, M. K., Umar, S. A., Chan, K. T., Latif, A. A., Azlan, M. N., Abubakar, A. I., & Hamza, A. M. (2019). Study of rice husk silicate effects on the elastic, physical and structural properties of borotellurite glasses. *Materials Chemistry and Physics*, *238*. https://doi.org/10.1016/j.matchemphys.2019.121891

Hamza, A. M., Halimah, M. K., Muhammad, F. D., & Chan, K. T. (2019). Physical properties, ligand field and Judd-Ofelt intensity parameters of bio-silicate borotellurite glass system doped with erbium oxide. *Journal of Luminescence*, *207*, 497–506. https://doi.org/10.1016/j.jlumin.2018.11.038

Hamza, A. M., Halimah, M. K., Muhammad, F. D., Chan, K. T., Usman, A., Faznny, M. F., Zaitizila, I., & Tafida, R. A. (2019). Structural, optical and thermal properties of Er3+-Ag codoped bio-silicate borotellurite glass. *Results in Physics*, *14*(March), 102457. https://doi.org/10.1016/j.rinp.2019.102457

Kaur, S., Pandey, O. P., Jayasankar, C. K., & Chopra, N. (2019). Spectroscopic, thermal and structural investigations of Dy3+ activated zinc borotellurite glasses and nano-glass-ceramics for white light generation. *Journal of*

Online ISSN: 2736-0903
Print ISSN: 2736-089X
www.slujst.edu.ng

Non-Crystalline Solids, *521*(May), 119472. https://doi.org/10.1016/j.jnoncrysol.2019.119472

Kundu, R. S., Dhankhar, S., Punia, R., Nanda, K., & Kishore, N. (2014). Bismuth modified physical, structural and optical properties of mid-IR transparent zinc boro-tellurite glasses. *Journal of Alloys and Compounds*, *587*, 66–73. https://doi.org/10.1016/j.jallcom.2013.10.141

Nazrin, S. N., Halimah, M. K., Muhammad, F. D., Yip, J. S., Hasnimulyati, L., Faznny, M. F., Hazlin, M. A., & Zaitizila, I. (2018). The effect of erbium oxide in physical and structural properties of zinc tellurite glass system. *Journal of Non-Crystalline Solids*, *490*(March), 35–43. https://doi.org/10.1016/j.jnoncrysol.2018.03.017

Polosan, S., Ganea, P., & Nitescu, A. (2021). Structural, magneto-optical and dielectric properties of phosphate tellurite glasses. *Materials Research Bulletin*, *143*(November), 111455. https://doi.org/10.1016/j.materresbull.2021.111455

Tanko, Y. A., Ghoshal, S. K., & Sahar, M. R. (2016). Ligand field and Judd-Ofelt intensity parameters of samarium doped tellurite glass. *Journal of Molecular Structure*, *1117*, 64–68. https://doi.org/10.1016/j.molstruc.2016.03.083

Umar, A., Yousef, E., & Lisiecki, R. (2018). Erbium-doped fl uorotellurite titanate glasses for near infrared broadband ampli fi ers. *Optical Materials*, *83*(June), 257–262. https://doi.org/10.1016/j.optmat.2018.06.020

Umar, S. A., Halimah, M. K., Chan, K. T., & Latif, A. A. (2017a). Physical, structural and optical properties of erbium doped rice husk silicate borotellurite (Er-doped RHSBT) glasses. *Journal of Non-Crystalline Solids*, *472*(June), 31–38. https://doi.org/10.1016/j.jnoncrysol.2017.07.013

Umar, S. A., Halimah, M. K., Chan, K. T., & Latif, A. A. (2017b). Polarizability , optical basicity and electric susceptibility of Er 3 + doped silicate borotellurite glasses. *Journal of Non-Crystalline Solids*, *471*(March), 101–109. https://doi.org/10.1016/j.jnoncrysol.2017.05.018

Usman, A., Halimah, M. K., Latif, A. A., Muhammad, F. D., & Abubakar, A. I. (2018). Influence of Ho3 + ions on structural and optical properties of zinc borotellurite glass system. *Journal of Non-Crystalline Solids*, *483*(December 2017), 18–25. https://doi.org/10.1016/j.jnoncrysol.2017.12.040